Plasmid-mediated phenotypic noise leads to transient antibiotic resistance in bacteria

SI: SUPPLEMENTARY FIGURES

Movie S1: MG/pBGT exposed to a semi-lethal pulse of AMP.
Movie S2: MG:GT exposed to a semi-lethal pulse of AMP.

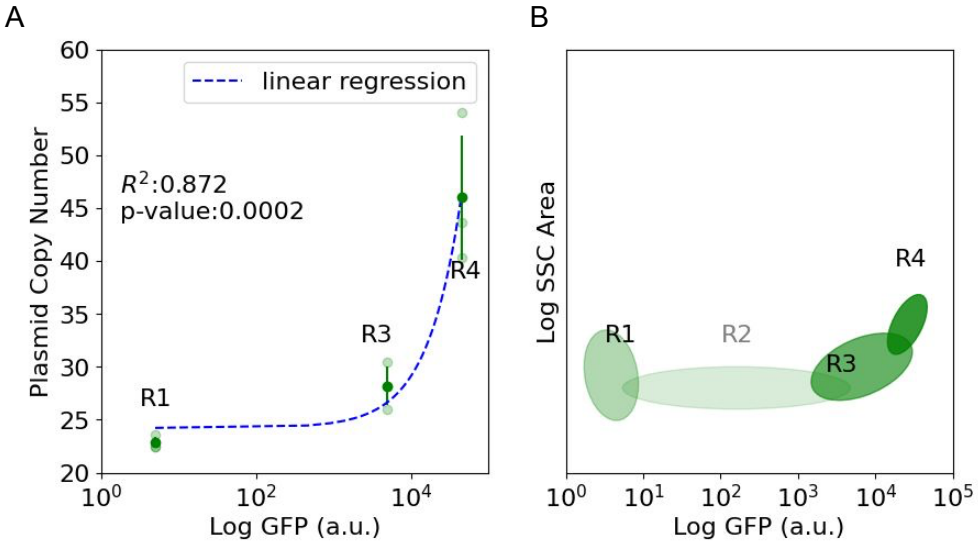

Figure S1. Correlation between PCN and fluorescent intensity. A) Positive correlation between GFP intensity and plasmid copy number estimated using qPCR, for different subpopulations obtained by sorting cells based on their fluorescent intensity. Mean and standard deviation (green) of three technical replicates (shaded green dots). A linear regression is depicted in the dashed blue line. B) Regions used to separate cells based on their fluorescent intensity using a flow cytometer cell sorter. Regions were defined based on standard side scatter area and GFP intensity.

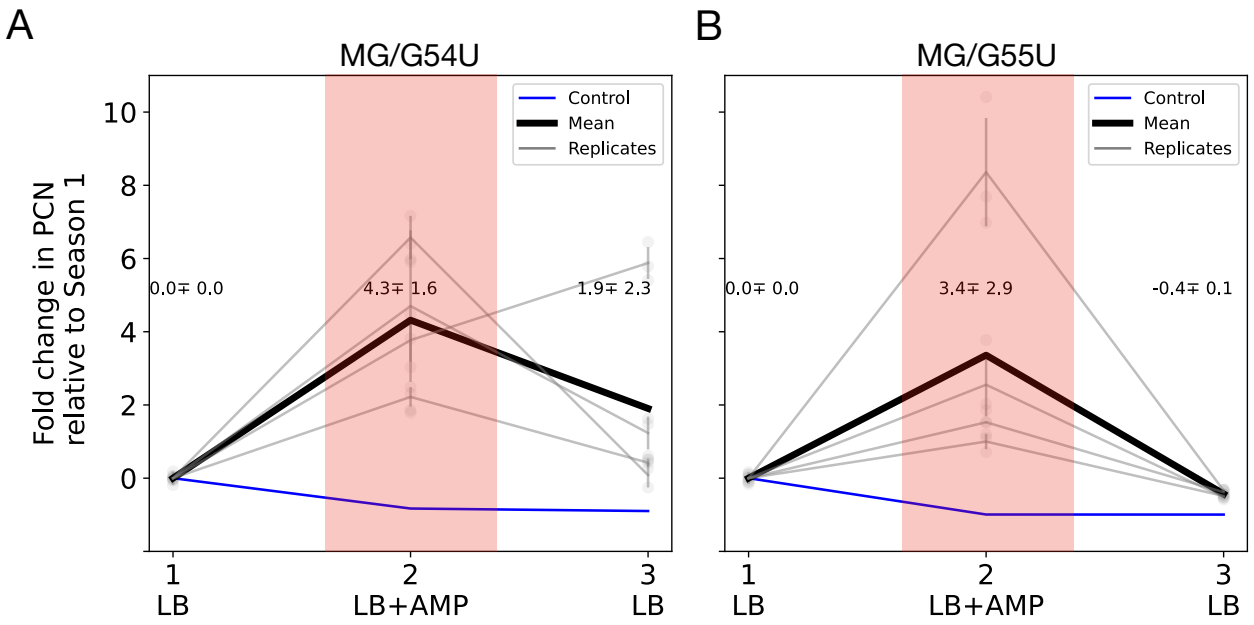

Figure S2. Rapid gene amplification is unstable in high-copy plasmids. A) Fold increase in PCN estimated using qPCR (relative to season 1) for strain MG/G54U in a three-season serial dilution experiment (black line represents the mean over $N = 4$ replicates, in grey). During the second season, a MIC of AMP is deployed (43 mg/ml), selecting for high-copy plasmid cells, therefore increasing five-fold the mean PCN in the population. In the third season, the antibiotic is removed and the mean PCN decrease to the levels exhibited prior to drug exposure. B) Mean PCN for MG/G55U also shows a rapid increase in fluorescence during drug exposure (46 mg/ml) and a rapid decline once the drug is removed.

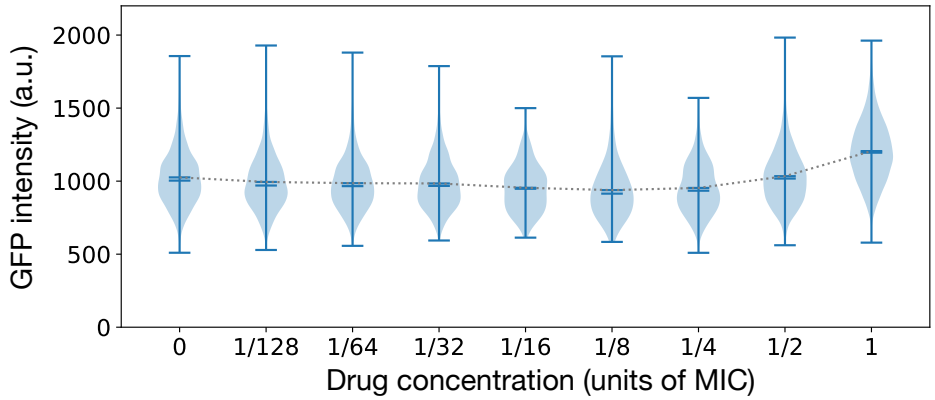

Figure S3. Mean fluorescence of GFP distributions remains constant in populations of MG:GT exposed to increasing concentrations of antibiotic.

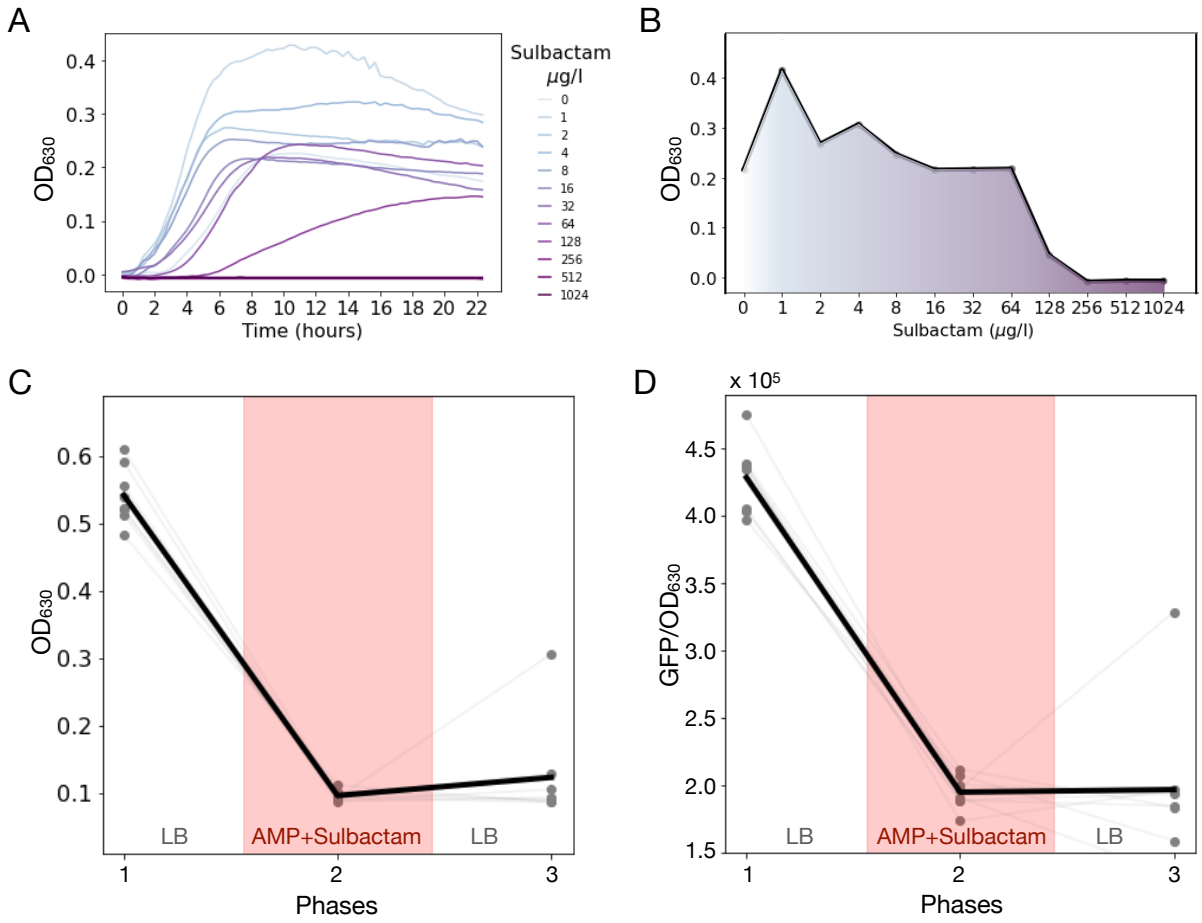

Figure S4. Survival assay with AMP and a β-lactamase inhibitor. A) Growth curves obtained for MG/pBGT populations exposed to 2 mg/ml of AMP and a range of sulbactam concentrations (low sulbactam doses in light blue, high concentrations in purple). B) Final optical density as a function of sulbactam concentration. We consider that bacterial growth is completely suppressed at concentrations higher than $256\mu g/l$ of sulbactam. C) Optical density (OD_{600}) measured after 12 hours of growth in a 3-season survival assay (season 1: LB; season 2: LB + sulbactam ($256\mu g/l$) + AMP ($2\ mg/ml$); season 3: LB). Gray lines represent different replicates ($N = 8$), with the mean OD_{600} represented with a black line. Of note, only one replicate exhibited growth after the recovery period. D) Normalized fluorescence intensity of populations exposed to a 3-season serial dilution experiment. Note that supplementing the media with sulbactam reduced the relative fluorescent intensity exhibited by the population during the drug exposure period, in contrast to previous experiments performed in the absence of sulbactam, where we observed an increase in fluorescence during AMP exposure.

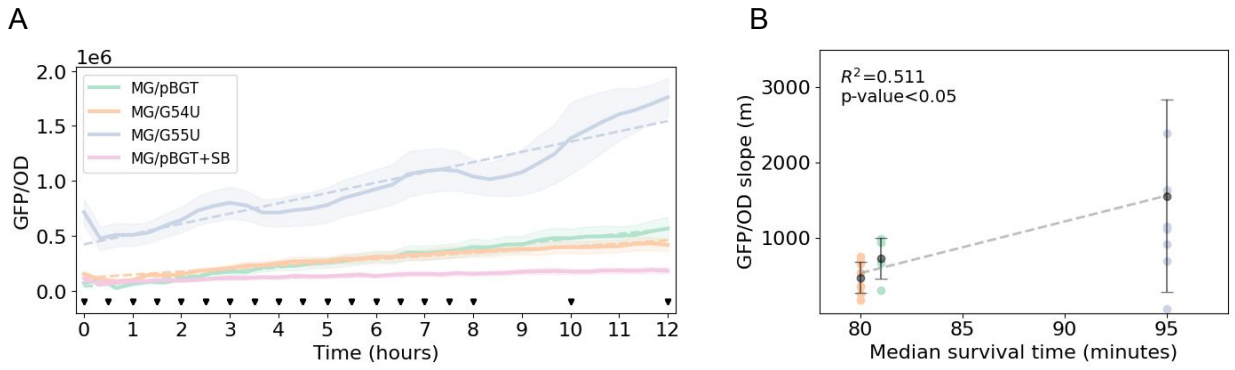

Figure S5. GFP response to antibiotics and survival. A) Per cell GFP fluorescence in different bacterial populations indicates that the increase in fluorescence is associated with the corresponding PCN of each population. Triangles at the bottom illustrate the sampling points used in the survival assay. B) Median survival time (duration of exposure that inhibits the population by 50%) shows a correlation with the observed increase in GFP for populations with different PCN.

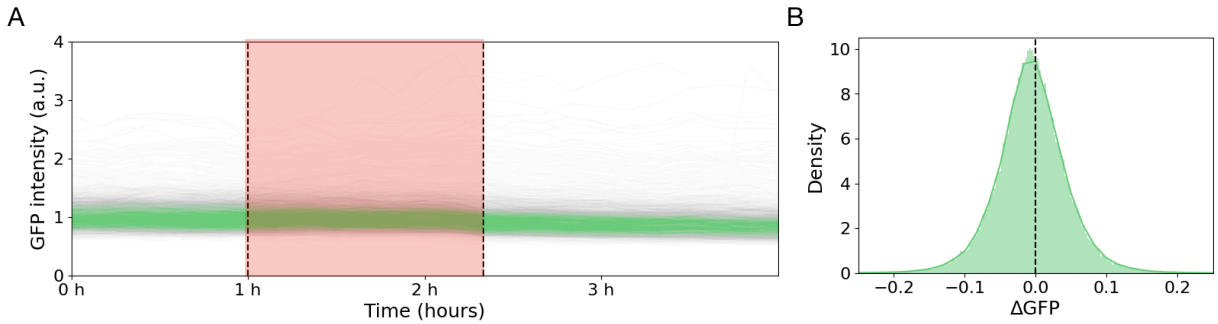

Figure S6. Single-cell time-series of GFP expression. A) GFP fluorescence as a function of time of surviving cells in the MG/pBGT population shows that fluorescent remains constant throughout the experiment. Red area denotes the interval of AMP exposure. B) Difference in GFP between consecutive frames (ΔGFP) during drug exposure. The symmetric distribution suggests there is no increase or decrease in GFP in response to AMP.

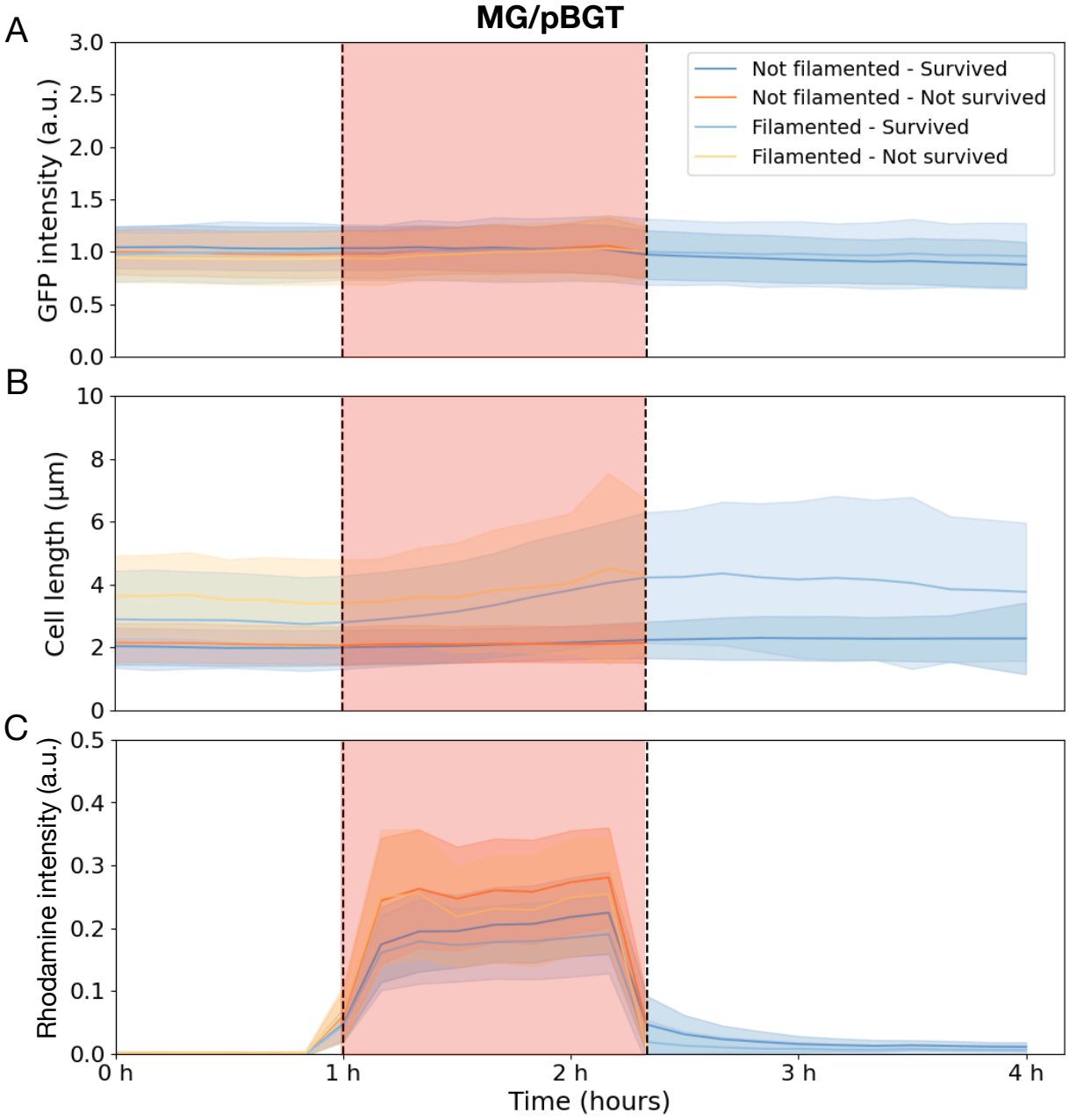

Figure S7. Population-level analysis of microfluidics data for MG/pBGT. A) Normalized GFP intensity as a function of time for different subpopulations: cells that survived (blue) and cells that did not survive (orange). Dark colors represent cells that filaments and light colors represent cells that did not filament. Shaded area representing the standard error over the mean. Red area denotes the duration of antibiotic exposure. B) Cell length as a function of time showing that filamented cells increased cell length during drug exposure. C) Fluorescent intensity in the red channel resulting from a fluorescent dye entering the cells during cell lysis.

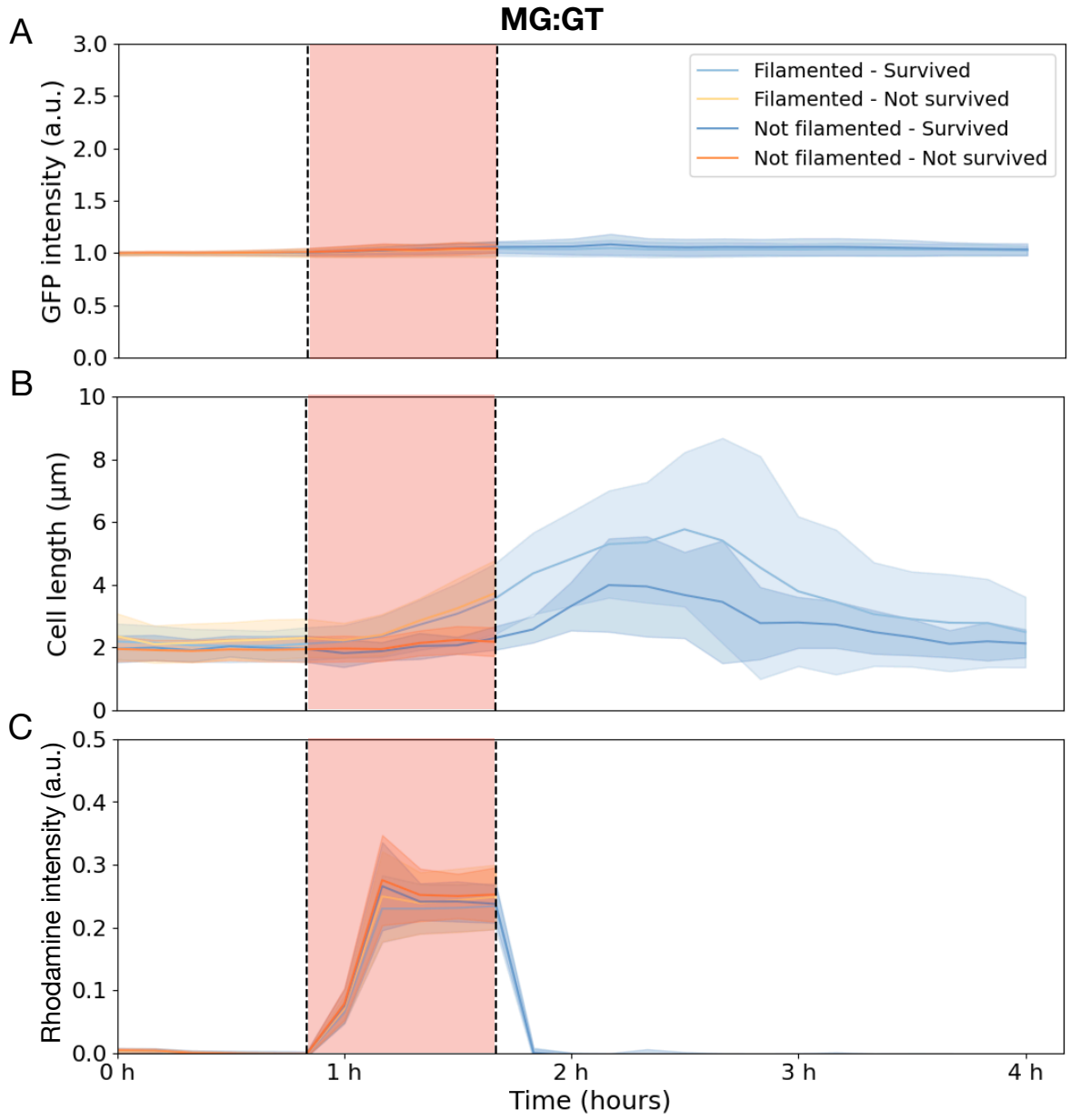

Figure S8. Population-level analysis of microfluidics data for MG:GT. A) GFP fluorescent intensity of MG:GT exhibits a stable expression over time, even in the presence of AMP (red area). B) Cell length as a function of time. During drug exposure, most surviving cells increased their cell length. C) Red fluorescent intensity inside each cell. Note a faster increase of fluorescent intensity for the non-surviving populations, consistent with an increase in the concentration of red fluorescent dye inside the cell.

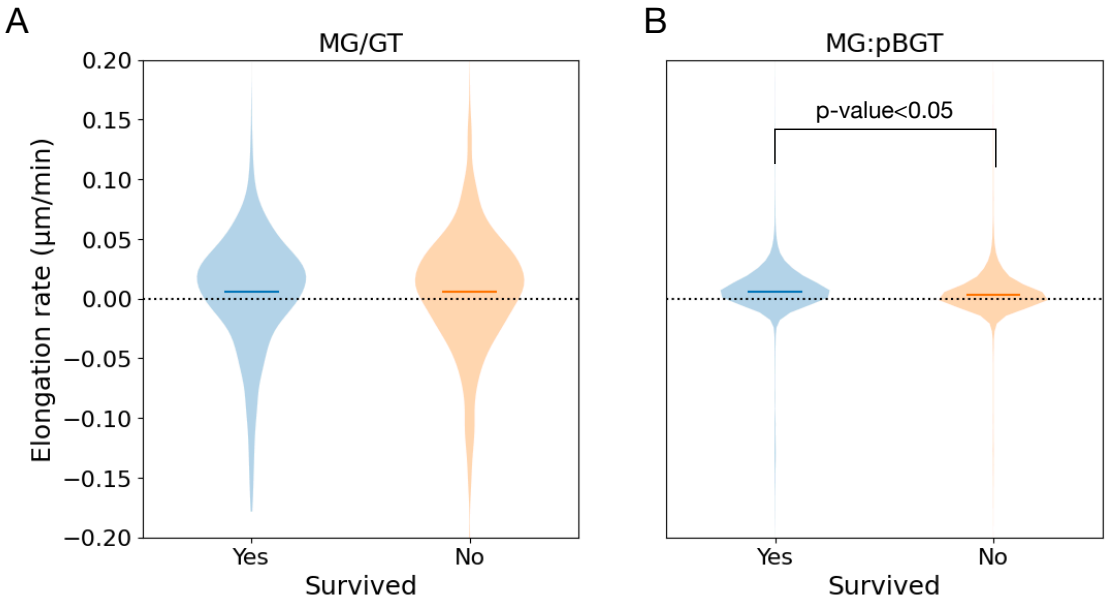

Figure S9. Single-cell elongation rates. Difference in cell length for individual cells in consecutive frames for cells that survived (blue) and did not survive (orange) drug exposure. A) Elongation rate for MG:GT cells. B) Elongation rate for MG/pBGT cells.

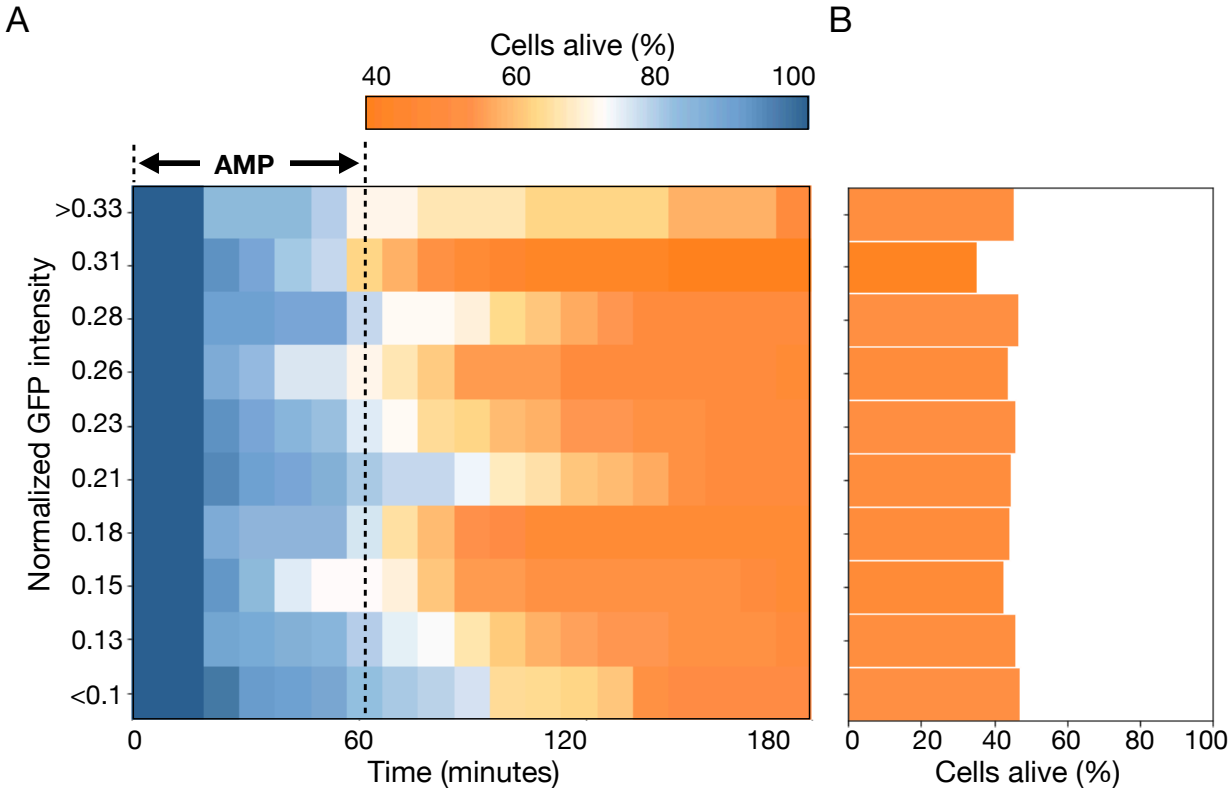

Figure S10. Survival rate and GFP intensity of MG:GT cells. A) Fraction of cells alive are denoted with a color gradient (from orange to blue) at different time-points. Dotted line illustrates the duration of the semi-lethal pulse. B) The percentage of cells that survive treatment remains constant regardless of the initial GFP intensity at the onset of drug exposure.

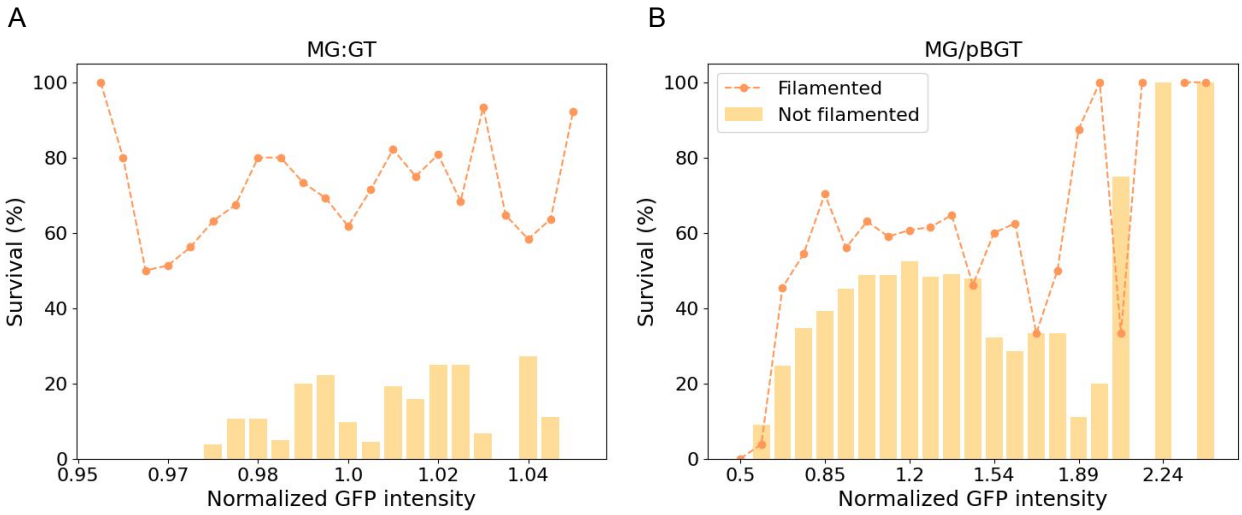

Figure S11. Survival probability of cells with different fluorescent intensities. A) Survival of MG:GT cells that did not produce filaments (bars) for different GFP intensities prior to drug exposure. Cells that filamented (orange lines) exhibited higher survival rates, regardless of their GFP intensity. B) Survival of MG/pBGT cells for different GFP intensities. Note that filamented cells also exhibited a higher survival rate. At higher fluorescent intensities, both filamented and non-filamented cells were able to transiently survive a pulse of a lethal concentration of AMP.

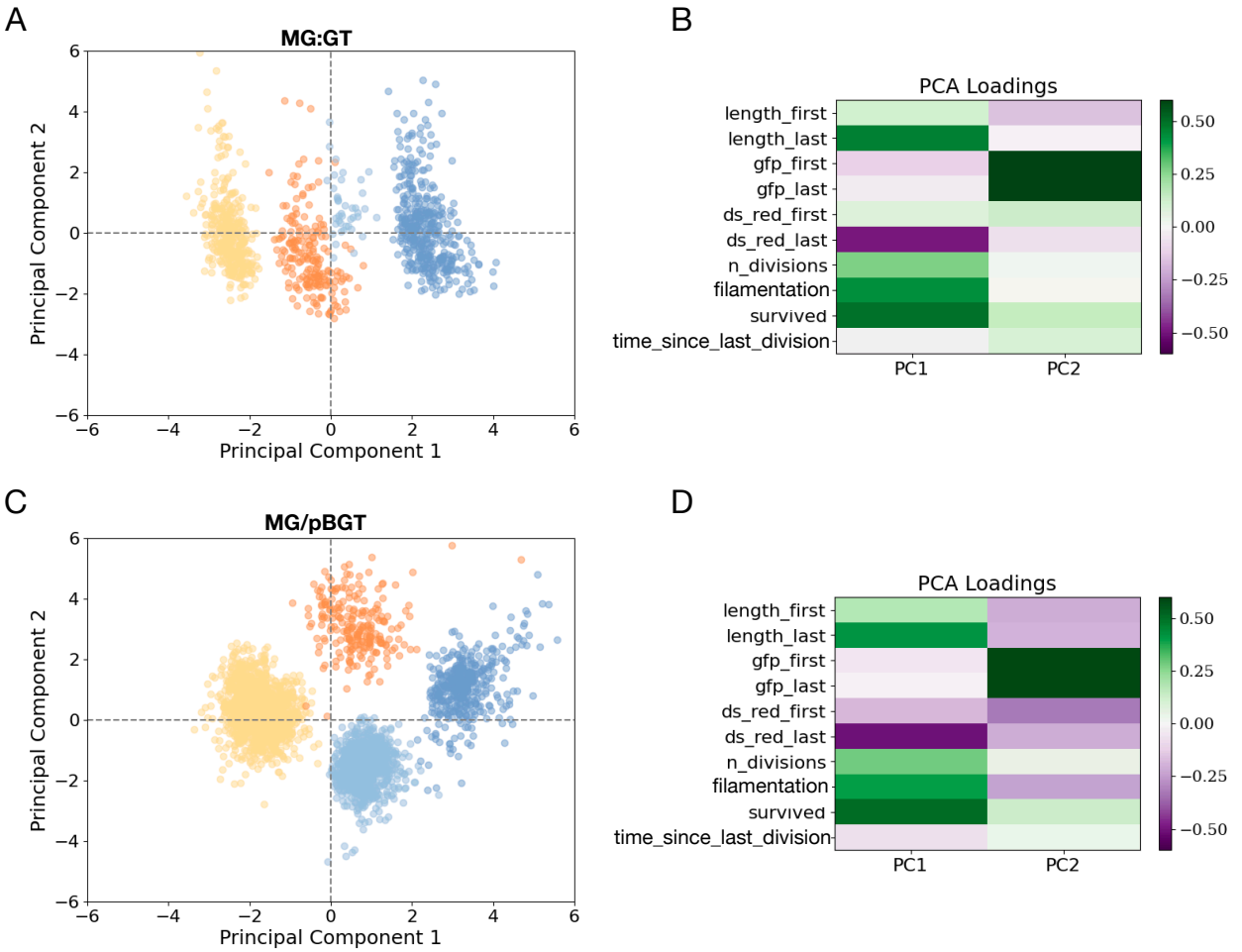

Figure S12. Principal Component Analysis shows the importance of cell length and GFP intensity in cell survival. A) The PCA plot shows the distribution of cells in the MG:GT population in a reduced dimensional space, where each point represents a sample and its position reflects its overall similarity to other samples based on multiple variables. The two axes of the plot correspond to the two principal components that explain the highest proportion of variance in the data. The color code indicates different subpopulations: cells that survived in blue and cells that were killed in orange. Dark colors represent cells that produced filaments and light colors cells where cell length was maintained. B) Individual contribution of each variable for the first two components of the PCA analysis. C) Dimensionality reduction analysis using PCA revealed distinct separation between surviving and antibiotic-killed cells, as well as between filamentous and non-filamentous cells, within the MG/pBGT population. D) PCA loadings associated with the MG:/pBGT population. For the first component, survival and the length of the cell explained most of the variability, while the second component was determined by the GFP intensity before and after drug exposure.

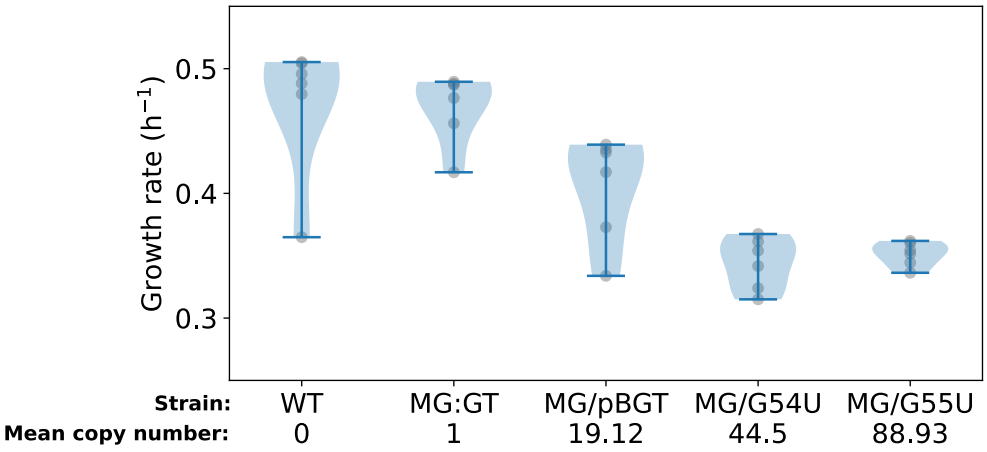

Figure S13. Fitness cost estimated at a population-level. Maximum growth rates estimated for different strains used in our study. There is a negative association between fitness in drug-free environments and the number of plasmids carried by each cell. A follow-up Tukey's Honest Significant Differences analysis yields the following strain pairs with p-value < 0.05 : WT-MG/pBGT, MG/pBGT-MG:GT, MG/pBGT-MG/G54U.

Strain ID	Mean PCN	AMP MIC ($\mu g/mL$)	Fitness (relative to MG)
MG	NA	4	1
MG:GT	NA	512	1.01
MG/pBGT	19.12 ± 1.53	$8,192$	0.943
MG/G54U	44.5 ± 3.81	$32,768$	0.793
MG/G55U	88.93 ± 15.65	$32,768$	0.557

Table S1. List of *Escherichia coli* MG1655 strains used in this study.

Parameter	Description	Value	source/rationale
μ	Mean plasmid copy number	19	Obtained from [1, **?**]
σ	Coefficient of variation max PCN	0.25	Value inferred from fluorescence data
Eff_i	Cell efficiency	1×10^6	This work *
V_{max}	Maximal uptake rate	2.5×10^{-8}	This work *
K_m	Half-saturation constant	0.25	This work *
p	Cost per plasmid	0.003	Table S1, $p = (1 - 0.943)/19$
ATP_{max}	Critical ATP concentration for division	1	This work *,**
δ	Antibiotic degradation	1×10^{-10}	Derived from [**?**]
B_0	Initial number of cells	1×10^3	1:1,000 bottle neck

Table S2. Parameter values employed in the numerical simulations of the agent-based model. * Values were adjusted based on the ODE model described in [**?**], modified to align with computational constraints, to maintain a maximum cell number, and to ensure cell divisions occur every 30 model iterations. ** Values set for ease of interpretation and visualization in the simulation results.